Magnetic and structural properties of $Mn(SCN)_2(CH_3OH)_2$: A quasi-two-dimensional Heisenberg antiferromagnet

G. C. DeFotis, E. D. Remy, and C. W. Scherrer
Chemistry Department, College of William and Mary, Williamsburg, Virginia 23185
(Received 11 July 1989; revised manuscript received 29 January 1990)

The magnetic behavior of $Mn(SCN)_2(CH_3OH)_2$ in single-crystal form has been studied, and the crystal structure has also been determined. The system is monoclinic, $C2/c$, $Z=4$ with $a=14.467(5)$ Å, $b=5.927(2)$ Å, $c=10.979(3)$ Å, and $\beta=93.19(3)°$. Manganese ions, of distorted octahedral coordination, are coupled together into quasi-two-dimensional arrays by bridging thiocyanate groups, and also by some hydrogen bonding. Potential interlayer-superexchange pathways are substantially less efficient, though probably not insignificant either. The magnetic properties seem consistent with the structural features. The single-crystal susceptibility exhibits uniaxial anisotropy in the paramagnetic regime, with χ_{a^*} somewhat larger than $\chi_b \approx \chi_c$. A broad maximum appears at 12.6(4) K in χ_b and χ_c, and a sharper maximum at 10.5 K in χ_{a^*}. An antiferromagnetic transition at 10.5(2) K is also apparent in the **b**- and **c**-axis susceptibilities, and below this temperature substantial anisotropies appear. A weak ferromagnetic moment develops along the **b** axis below 10.5 K, and from the magnitude of the spontaneous moment along this axis it is deduced that the spins are canted 0.20° from the **c** axis toward **b**. A possible spin-reorientation transition at 3.7_5 K is also apparent. High-temperature series-expansion fits to the susceptibilities suggest that a two-dimensional Heisenberg model is appropriate, but that interlayer exchange cannot be neglected; derived parameters are $J/k=-0.70(3)$ K and $J'/k=-0.16(2)$ K. The anisotropy observed in the paramagnetic regime suggests that a rather strong single-ion anisotropy of the form $D[\hat{S}_z^2-S(S+1)/3]$, with $D/k=0.29(2)$ K, is also present. The results are compared with various theoretical predictions for two-dimensional and three-dimensional models, and it appears that the system is more or less intermediate between these two lattice dimensionalities. The canting that is observed is almost certainly due to site-inequivalent single-ion anisotropy rather than to antisymmetric exchange. A detailed consideration of intralayer- and interlayer-superexchange pathways is also presented, and rather satisfactorily accounts for the observed differences in exchange interactions between this system and the analogous ethanol compound.

I. INTRODUCTION

Insulating magnetic systems of low lattice dimensionality, that is, one-dimensional (1D) or linear-chain systems and two-dimensional (2D) or layer systems, have been studied extensively for at least three decades.[1] The majority of the emphasis probably has been on 1D systems, since apart from the minimal realistic lattice dimensionality of this case, a number of special features peculiar to or accentuated in 1D systems can occur, e.g., spin-Peierls transition, alternating spin chain, solitons, bound magnons, the Haldane conjecture, etc.[2] Moreover, 1D theoretical models are much more often exactly solvable, or nearly so, than models of higher lattice dimensionality. Nevertheless, 2D systems continue to be of substantial interest from several points of view, e.g., obtaining examples of unusual models such as 2D-XY (which may exhibit a Kosterlitz-Thouless magnetic phase transition), studying magnetic phase diagrams for this particular dimensionality, and elucidating magnetostructural correlations within and between layers. Most recently of course, two-dimensional Heisenberg-model antiferromagnetism has become of special interest in connection with high-temperature superconductivity in layered copper oxide materials.

We have been studying[3-5] a family of predominantly 2D magnetic systems of the general type $M(SCN)_2(ROH)_2$, where M is a divalent transition metal ion (Mn^{2+},Fe^{2+},Co^{2+},Ni^{2+}) and where various alcohols ($R=CH_3$,C_2H_5, i-C_3H_7,n-C_3H_7) can also occur. There is a potential for obtaining new examples of 2D-Ising and 2D-XY magnets among the more anisotropic members (primarily Fe^{2+} and Co^{2+}) of this family, as well as for exercising some control over the strength of the interlayer interaction, and so the degree of two-dimensionality, by varying the alcohol group in a series based on a particular metal ion. Also the polynuclear thiocyanate ion is a relatively little utilized superexchange ligand, even though interactions mediated by it can be substantial. Additional systems involving SCN^- should be useful in furthering the understanding of magnetostructural correlations involving this superexchange bridge, and perhaps also in systems involving polynuclear superexchange ligands in general.

In this paper we describe the crystal structure and examine the single-crystal magnetic behavior of $Mn(SCN)_2(CH_3OH)_2$. The only member of the manganese series in this family of compounds previously studied in single-crystal form is $Mn(SCN)_2(C_2H_5OH)_2$.[6] It was shown to be a 2D Heisenberg antiferromagnet ex-

hibiting a canted spin arrangement and weak ferromagnetism below an ordering temperature of 10.30 K. In the following it emerges that the structure and magnetic properties of the methanol homologue bear a number of similarities to those of the ethanol system, but also some significant differences. In particular, interlayer exchange is substantially stronger, so that certain 3D characteristics are evident; nevertheless, the system remains predominantly two-dimensional in its behavior.

II. EXPERIMENTAL

Anhydrous $Mn(SCN)_2$ was prepared as described previously,[7] then dissolved in spectroscopic grade methanol and slowly evaporated in a dessicator over 3-Å molecular sieves. Crystals of $Mn(SCN)_2(CH_3OH)_2$ were obtained, pale green in color and often in the form of relatively flat diamond-shaped prisms. Chemical analysis confirmed their chemical composition. The crystals cleaved easily parallel to the large flat face, similar to the behavior described for $Mn(SCN)_2(C_2H_5OH)_2$, suggesting a structure based on layers weakly coupled together chemically. Measurements of interfacial angles and comparison with predictions from the crystal structure (see the next section) implied that, again as for the ethanol system, the crystal faces were those of the {011} and {100} forms, with the *b-c* plane the large flat face. The implicit identification of the monoclinic *b* axis by this method, a short diagonal in the diamond face, was confirmed by x-ray analysis. The single crystal used in the magnetic measurements weighed 18.21 mg. To protect it during measurements, from either water absorption or loss of alcohol, it was coated with a thin layer of apiezon grease.

Magnetization and susceptibility measurements were made using a variable-temperature vibrating-sample-magnetometer system described previously.[8] Temperatures, measured with a carbon-glass resistance thermometer in close proximity to the sample, are estimated to be accurate to ±0.010–0.20 K, depending on the range, with a precision substantially better than this. Magnetization and susceptibility data are estimated to be accurate to within 1.5%, also with a precision substantially better yet. Susceptibilities displayed in the following have been corrected for diamagnetism and demagnetization. Magnetic-field values are accurate to max(2 G, 0.1%). A small power supply, external to the main power supply and field-control unit, was used to cancel most of the residual field from the 12-in. electromagnet for the purpose of making low-field measurements.

III. CRYSTAL STRUCTURE

Manganese thiocyanate dimethanol, $Mn(SCN)_2(CH_3OH)_2$, is found to crystallize in the monoclinic space group $C2/c$, with $Z=4$, $a=14.467(5)$ Å, $b=5.927(2)$ Å, $c=10.979(3)$ Å, and $\beta=93.19(3)°$ [at 20±1 °C, using λ(Mo $K\alpha$)=0.71073 Å]. The volume of the unit cell is 939.9(6) Å^3 and the calculated density is 1.662(1) g cm^{-3}.[9]

Unit cell parameters were determined by a least-square refinement of the angular settings of 15 reflections beyond $2\theta=15°$. A total of 870 independent reflections were measured in the range $3.0° \leq 2\theta \leq 50.7°$, and 568 of these, with intensities at least three times their standard deviations, were used in the detailed structure analysis. Empirical absorption corrections were made using the psi-scan method based on seven reflections; relative transmission factors ranged from 0.416 to 1. Neutral-atom scattering factors were used, and anomalous dispersion corrections were made for the Mn and S atoms.[10]

Mn atoms were placed at centers of symmetry [special position (c)], and a heavy-atom Patterson technique was used to locate all the nonhydrogen atoms. The structure was refined, assuming isotropic thermal parameters, to $R=0.106$. Allowing for the expected anisotropic thermal motion reduced R to 0.063. Hydrogen atoms were then located and refined, isotropically, by difference Fourier synthesis, leading to a final R value of 0.041. There were no peaks present in the final difference Fourier map above the background level of 0.37e/Å^3.

Fractional coordinates and thermal parameters for various atoms appear in Table I. Selected bond distances and bond angles appear in Table II. A tabulation of observed and calculated structure factors is available upon request.

Manganese ions are coordinated octahedrally to four

TABLE I. Fractional atomic coordinates and thermal parameters (Å^2) for $Mn(SCN)_2(CH_3OH)_2$. The numbers in parentheses are the estimated deviations in the last significant digits. Atoms are labeled in accordance with Fig. 1.

Atom	X	Y	Z	B_{11} or B_{iso}	B_{22}	B_{33}	B_{12}	B_{13}	B_{23}
Mn	0.2500	0.2500	0	3.8(1)	2.1(1)	1.6(1)	−0.7(1)	−0.4(1)	0.3(1)
N	0.2075(4)	0.5974(8)	0.3298(4)	4.3(3)	2.8(2)	2.1(2)	−0.1(2)	0.0(2)	−0.5(2)
C1	0.1710(4)	0.5581(8)	0.2354(4)	2.8(3)	1.8(2)	2.0(2)	−0.1(2)	0.4(2)	−0.1(2)
S	0.1170(1)	0.5031(3)	0.1029(1)	3.9(1)	2.9(1)	2.1(1)	−0.2(1)	−0.5(1)	−0.3(1)
O	0.3500(4)	0.5176(8)	0.0338(4)	4.5(2)	2.6(2)	3.3(2)	−1.1(2)	−1.1(2)	0.6(2)
H_0	0.3427(52)	0.6182(116)	−0.0111(62)	5(2)					
C2	0.4212(5)	0.5416(12)	0.1292(6)	4.2(4)	3.8(3)	4.2(3)	−1.0(3)	−1.1(3)	0.1(3)
H_{2a}	0.4580	0.6762	0.1276	4.9[a]					
H_{2b}	0.4605	0.4118	0.1251	4.9					
H_{2c}	0.3891	0.5371	0.2034	4.9					

[a]Methyl hydrogens were located and refined relative to C2 rather than independently.

TABLE II. Bond distances and bond angles in $Mn(SCN)_2(CH_3OH)_2$. The numbers in parentheses are the estimated deviations in the last significant digits. Atoms are labeled in accordance with Fig. 1.

Bond	Distance (Å)	Bond	Distance (Å)
Mn—S	2.733(2)	Cl—N	1.160(7)
Mn—O	2.165(5)	O—C2	1.434(8)
Mn—N″	2.135(4)	O—H_o	0.78(7)
S—Cl	1.646(5)	C2—H_2	0.96

Bond	Angle (deg)	Bond	Angle (deg)
S—Mn—O	90.3(1)	Mn—S—C1	99.4(2)
S—Mn—N″	92.6(1)	Mn—O—C2	130.1(4)
O—Mn—S′	89.7(1)	Mn—O—H_o	113(5)
O—Mn—N″	90.2(2)	C2—O—H_o	117(5)
S′—Mn—N″	87.4(1)	Mn—N″—Cl″	164.0(5)
O′—Mn—N″	89.8(2)	S—Cl—N	178.7(6)
S—Mn—S′	180.0		
O—Mn—O′	180.0		
N″—Mn—N‴	180.0		

SCN^- groups and a pair of methanols; see Fig. 1. The SCN groups are, as expected, essentially linear with an S—C—N angle of 178.7(6)°. The Mn—N—C angle is only 16° from being linear, and the Mn—S—C angle is roughly tetrahedral. SCN^- groups link manganese ions together, forming infinite polymeric sheets parallel to the *b-c* plane. This can be seen from an examination of Figs. 2 and 3, where the relative isolation of *b-c* layers is also evident. Figure 4 is a view of the *b-c* plane itself; the extension over the area of several unit cells clearly illustrates the SCN-coordinated network of manganese ions. The situation is rather similar to that found in $Mn(SCN)_2(C_2H_5OH)_2$.[6]

Within a *b-c* layer the nearest-neighbor and next-nearest-neighbor manganese ions are 5.927 and 6.238 Å apart. The analogous intralayer separations in $Mn(SCN)_2(C_2H_5OH)_2$ are 6.313 and 6.339 Å. Thus the polymeric sheets are a bit more tightly packed in the methanol system. The separation between *b-c* layers is

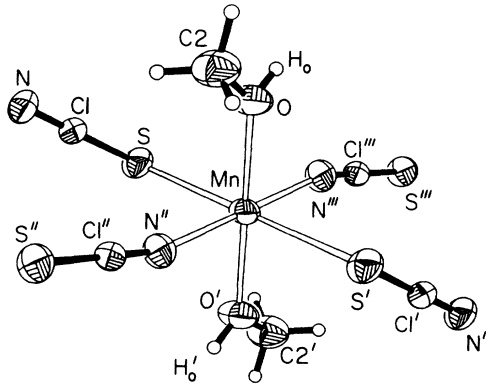

FIG. 1. Coordination geometry about a manganese ion in $Mn(SCN)_2(CH_3OH)_2$. Atom labeling corresponds to that in Tables I and II and in text.

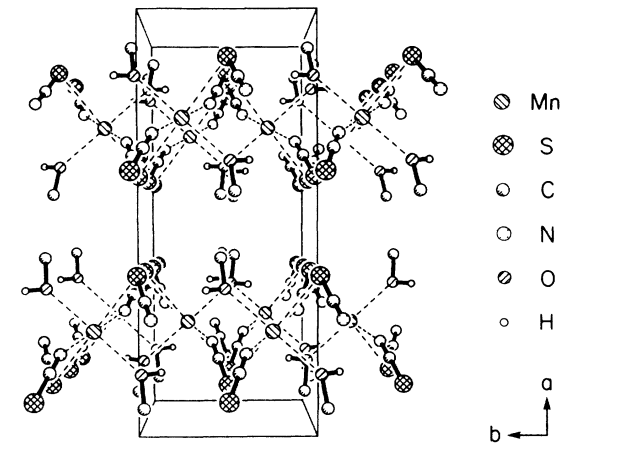

FIG. 2. Perspective view of the unit cell of $Mn(SCN)_2(CH_3OH)_2$ along the *c* axis. Methyl group hydrogens are omitted.

7.222 Å in $Mn(SCN)_2(CH_3OH)_2$; the corresponding separation in $Mn(SCN)_2(C_2H_5OH)_2$ is 8.507 Å. Thus the packing normal to the layers is also somewhat tighter in the methanol system, and its density, 1.662 $g\,cm^{-3}$, is, despite the lower molecular weight, significantly greater than that of the ethanol system, 1.485 $g\,cm^{-3}$. The separation between nearest-neighbor manganese ions in adjacent layers of $Mn(SCN)_2(CH_3OH)_2$ is 7.817 Å; in the ethanol system the corresponding separation is 8.535 Å. Further comparisons between the structures of $Mn(SCN)_2(CH_3OH)_2$ and $Mn(SCN)_2(C_2H_5OH)_2$ will be postponed until Sec. VI.

IV. MAGNETIC MEASUREMENTS

The magnetic behavior of members of the manganese subseries in polycrystalline form were reported recently.[4] For $Mn(SCN)_2(CH_3OH)_2$ high-temperature susceptibility data were Curie-Weiss-like $[\chi_M = C/(T-\Theta)]$, with

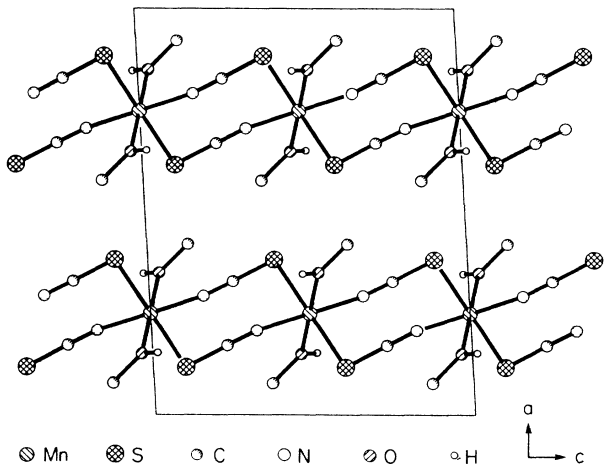

FIG. 3. Projective view of the unit cell of $Mn(SCN)_2(CH_3OH)_2$ along the *b* axis. Methyl group hydrogens are omitted.

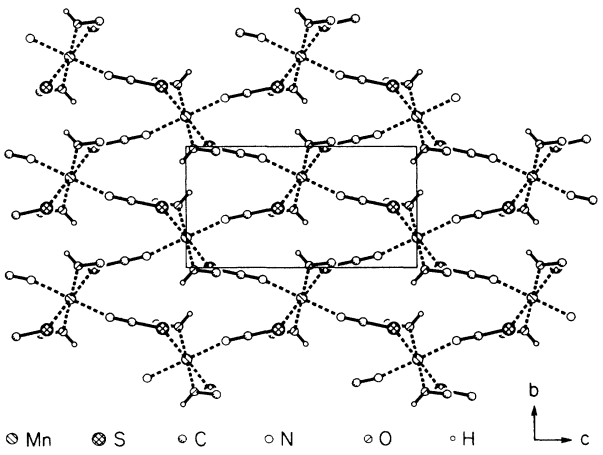

FIG. 4. Projective view of the *b-c* plane of $Mn(SCN)_2(CH_3OH)_2$ extended over several unit cells. Methyl group hydrogens are omitted.

$g=1.99\pm0.01$ [$C=N_0g^2\mu_B^2S(S+1)/3k$ with $S=\frac{5}{2}$] and $\Theta=-22.4\pm0.4$ K. A broad maximum in the susceptibility occurred at 12.6 ± 0.4 K, with $\chi_{max}=0.107\pm0.001$ emu/mole. The intralayer exchange was estimated from the susceptibility data in various ways, with values ranging from $J/k=-0.70\pm0.03$ to -0.77 ± 0.02 K depending on the method. The exchange Hamiltonian is taken as $-2\sum_{i>j}J\hat{\mathbf{S}}_i\cdot\hat{\mathbf{S}}_j$, a negative J indicating an antiferromagnetic interaction.

In Fig. 5 we show the molar magnetic susceptibility of single-crystal $Mn(SCN)_2(CH_3OH)_2$. Measuring fields used were 2400 and 4200 G, depending on the temperature range, with the observed magnetization confirmed to be essentially linear in applied field. Along the monoclinic *b* axis a broad maximum occurs at 12.6 ± 0.4 K, with $\chi_{max}=0.102\pm0.001$ emu/mole. Such a feature is characteristic of antiferromagnets with lattice dimensionality lower than three. At 10.5 ± 0.2 K a marked increase in the susceptibility occurs, clearly signalling the onset of a magnetic phase transition. That χ increases sharply along this axis suggests that some degree of ferromagnetic alignment is occurring. One also notices a definite change in slope of $\chi(T)$ at about 3.75 ± 0.2 K, below which the susceptibility increases markedly faster with decreasing temperature.

Along the monoclinic *c* axis a similar broad maximum occurs, also centered at about 12.6 K, with $\chi_{max}=0.103\pm0.001$ emu/mole. Here χ continues merely to decrease through the 10.5-K transition. Close examination of an expanded scale plot containing more numerous data reveals, however, a probable maximum in $\partial\chi/\partial T$ at 10.5 K. Such a feature has been proved to occur at the transition temperature in the parallel susceptibility of an antiferromagnet;[11] apart from the low-temperature upturn, the *c*-axis data are most reminiscent of a parallel susceptibility. There is some indication of an anomaly near 3.75 K along this axis also, below which χ increases somewhat more rapidly with decreasing temperature.

Along the a^* axis, normal to the *b-c* layers of the manganese ions, the susceptibility is substantially larger than along the two orthogonal directions, at any rate below about 25 K. Along this axis a somewhat sharper maximum is seen at 10.5 K, with $\chi_{max}=0.121\pm0.001$ emu/mole. Just below 9.2 K χ begins to increase with decreasing temperature. For this axis no anomaly near 3.75 K is discernible. However, it is interesting to note that the susceptibility crosses and becomes a bit larger than that along *b* at a temperature of about 3.5 K, just slightly below the 3.75-K anomalies along the other axes. At 12.6 K the average value of the a^*-, *b*-, and *c*-axis susceptibilities is 0.107 ± 0.002 emu/mole, in agreement with the powder value.

Since the behavior along the *b* axis gives some evidence for weak ferromagnetism, the magnetization was remeasured in a much smaller field. The result at a measuring field of 100 G appears in Fig. 6. Above 10.5 K the magnetization has a small and somewhat imprecisely determined value (because of the small size of the signal). At 10.5 K a sharp increase occurs, and at lower temperatures M gradually approaches a value around 112

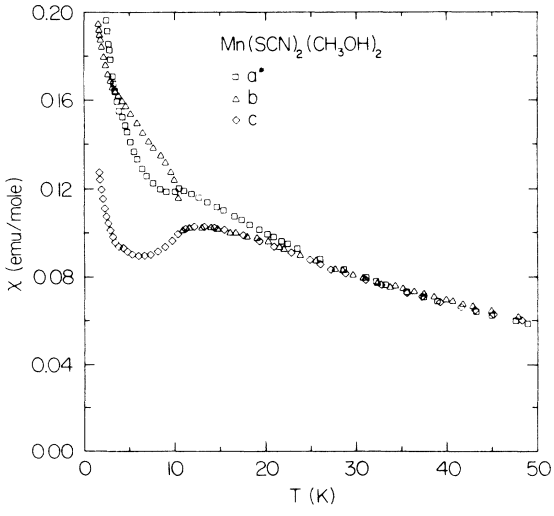

FIG. 5. Molar susceptibility vs temperature along three orthogonal crystal axes of $Mn(SCN)_2(CH_3OH)_2$. Applied magnetic field is either 2400 or 4200 G, depending on the temperature range.

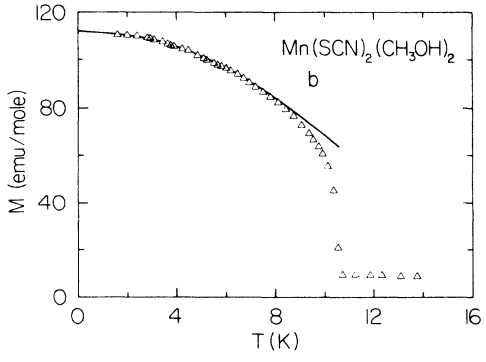

FIG. 6. Molar magnetization vs temperature along the *b* axis of $Mn(SCN)_2(CH_3OH)_2$ in a 100-G field. Curve through data is a spin-wave theory fit described in Sec. V A of text.

emu/mole near 0 K, which represents the spontaneous magnetization along b plus a much smaller field-induced magnetization. It is somewhat uncertain whether any anomaly appears in these low-field data in the region just below 4 K. Clearly though, the strong low-temperature upturn evident in the higher-field data of Fig. 5 is not present.

Further evidence of the weak ferromagnetism along b is evident from Fig. 7, where the magnetization is shown as a function of applied field at two temperatures for each axis. In each case one sees a linear or nearly linear relation between M and H at 4.22 K, with departures from linearity least for the c axis and greatest for the a^* axis. This temperature is well below the 10.5-K magnetic ordering transition inferred from the susceptibility data, but above the apparent anomaly at 3.75 K seen along the b and c axes. Only along the b axis does an extrapolation of the magnetization to $H=0$ (see inset) yield a nonzero value, $M_0=93.2$ emu/mole at 4.22 K. At 1.84 K this remains the case; $M_0=96.8$ emu/mole along b and zero for the other two axes. Now, however, a distinct nonlinearity of M versus H is evident for each axis, for fields in excess of several kG. It is tempting to relate this to the fact that the temperature is below the 3.75 K of the susceptibility anomaly. The absence of any signs of field-induced phase transitions in the data of Fig. 7 implies that any spin-flop transition in $Mn(SCN)_2(CH_3OH)_2$ occurs only at a field larger than the 16-kG limit of our magnet.

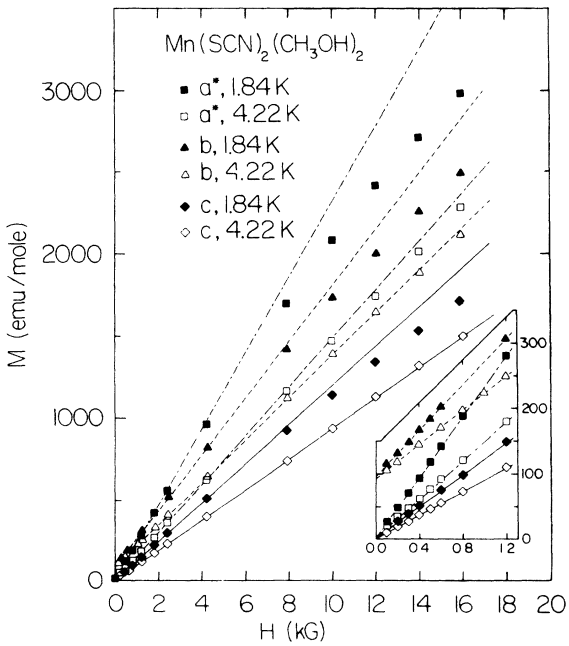

FIG. 7. Molar magnetization vs field along three orthogonal crystal axes of $Mn(SCN)_2(CH_3OH)_2$ for two different temperatures. Straight lines are drawn through low-field data and extended to higher fields. Inset is an expanded view of the low-field region.

V. ANALYSIS

A. Magnetization data and ordered state

It is possible to estimate the degree of spin canting necessary to produce the observed weak ferromagnetic moment along b. Assume that the manganese spins order almost parallel and antiparallel to c, but that those of each sublattice are canted slightly toward the b axis below the spontaneous ordering temperature of 10.5 K. From Fig. 7 (inset) one sees that M_0 along b varies only slightly between 4.2 and 1.8 K, as expected for temperatures less than $T_N/2$, and little further increase in the 96.8-emu/mole value as $T\rightarrow 0$ can be anticipated. The full saturation moment of a mole of manganese spins is

$$N_0 g\mu_B S = N_0(5.00\mu_B/\text{ion}) = 27.93\times 10^3 \text{ emu/mole} .$$

The ratio $M_0/M_{\text{sat}}=0.003\,47$ corresponds to $\sin\phi$ where ϕ is the angle by which the moments are canted from c. The result is $\phi=0.20°$.

The detailed temperature dependence of M_b in a small 100-G field should be rather similar to that of the spontaneous magnetization. The magnetization data of Fig. 6 are found to conform rather well (rms deviation $\approx 0.4\%$) to

$$M = M_0(1-AT^2) , \tag{1}$$

with $M_0=112$ emu/mole and $A=0.0038\pm 0.0002$ K^{-2}, in the temperature range 1.8 to 6.5 K ($0.62T_N$). The fitted curve also appears in Fig. 6. This is the expected form, neglecting higher-order terms in T and neglecting anisotropy effects, for the sublattice magnetization of an antiferromagnet according to spin-wave theory.[12] Since we are measuring the weak ferromagnetic moment arising from canting of the antiferromagnetic sublattices, it may be wondered whether a form similar to Eq. (1) but with $T^{3/2}$ rather than T^2 is more germane, as observed in ferrimagnets and ferromagnets. We find, however, that such a $T^{3/2}$ form provides a much worse fit to the data in the 3.5–6.5-K range, and is also significantly less satisfactory in the range below 3.5 K.

Assuming that Eq. (1) is appropriate and applicable to as high as 62% of T_N, one can estimate the antiferromagnetic exchange interaction strength from the coefficient A. Employing the expression for A in Ref. 12, and using values of certain parameters in that expression appropriate to a face-centered cubic lattice (more akin to the monoclinic $Z=4$ structure of our system than is a simple cubic lattice), one finds that $A=0.000\,52\,(k/|J|)^2$, with the same convention for J as given in Sec. IV. From the fitted A value one finds that $|J/k|=0.37\pm 0.02$ K.

B. Susceptibility data and paramagnetic state

One advantage of the single-crystal data is that the rounded maximum in χ is better formed, at any rate for the c-axis data, then in powder measurements. The structure is such that each manganese ion is connected to four

other manganese ions in a layer via bridging SCN^- groups. Since Mn^{2+} is usually a rather isotropic ion, it is natural to apply a 2D Heisenberg model to the present system. Two relations which have been obtained from analysis of high-temperature series expansions (HTSE's) for the 2D (square-planar)-Heisenberg model with $S=\frac{5}{2}$ are[1(a)]

$$kT(\chi_{\max})/|J|S(S+1)=2.05\pm0.01 , \quad (2)$$

$$\chi_{\max}|J|/N_0g^2\mu_B^2=0.0551\pm0.0001 , \quad (3)$$

where $T(\chi_{\max})$ is the temperature at which the susceptibility attains a maximum, the exchange Hamiltonian is that given earlier, and the other symbols have their usual meanings. If one substitutes the value $T(\chi_{\max})=12.6\pm0.4$ K into Eq. (2), the value $J/k=-0.70\pm0.03$ K results. If one substitutes the value $\chi_{\max}=0.103\pm0.001$ emu/mole into Eq. (3), and takes $g=2.00$ (virtually always so for Mn^{2+} systems, and consistent with high-temperature Curie-Weiss behavior in this system), the value $J/k=-0.80\pm0.01$ K results. Thus, it appears that the magnitude of $\chi_{\max}$ is somewhat less than expected based on its location along the T axis. This suggests the presence of significant antiferromagnetic interlayer interactions.

Alternatively, the HTSE for the 2D (square-planar)-Heisenberg model can be used to fit $\chi(T)$ directly. As given for general S in Ref. 13, it is of the form

$$N_0g^2\mu_B^2/\chi_M J=3\Theta+\sum_{n=1} C_n/\Theta^{n-1} , \quad (4)$$

where the exchange Hamiltonian is $\sum_{i>j} J\hat{\mathbf{S}}_i\cdot\hat{\mathbf{S}}_j$, and where $\Theta=kT/JS(S+1)$. In the results that follow, on applying this series to the c-axis data, we express J values in the convention previously noted

$$\hat{\mathcal{H}}_{ex}=-2\sum_{i>j} J\hat{\mathbf{S}}_i\cdot\hat{\mathbf{S}}_j .$$

If g is fixed at 2.00, a best-fit (rms deviation=3.4%) value of $J/k=-0.81_7$ K results when only data in the 11–50-K range are used; see Fig. 8. Including data (not appearing in Fig. 8) to 300 K leads to a best-fit (rms deviation=5.7%) value of $J/k=-0.83_7$ K, only slightly different. Increasing the minimum fitted temperature to 12 K yields J values only 1% or less different (slightly more negative). The J values are similar to that estimated from the size of $\chi_{\max}$ and in less good agreement with that estimated from the location of $\chi_{\max}$. However, neither fit can be considered really satisfactory. If g is allowed to vary, much better fits are obtained: $g=1.91_6$, $J/k=-0.73_6$ K, rms deviation=0.44%, for 11–50-K data (see Fig. 8); and $g=1.92_0$, $J/k=-0.74_3$ K, rms deviation=0.54%, for 11–300-K data. Now J/k is more consistent with the value estimated directly from the location of $\chi_{\max}$ and less so with the value estimated from the magnitude of $\chi_{\max}$. However, the g values are too low to be credible for a Mn^{2+} compound.

It is certainly plausible that the failure to achieve fully satisfactory fits with $g=2.00$ fixed may be due to deviations from strictly 2D magnetic behavior. The effects of

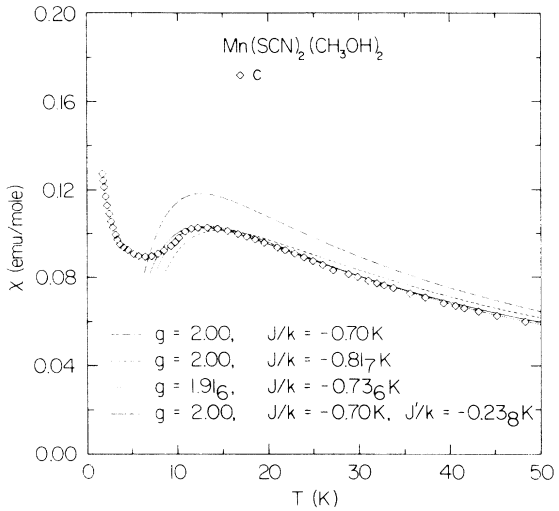

FIG. 8. Molar susceptibility vs temperature along the c axis of $Mn(SCN)_2(CH_3OH)_2$, and various theoretical fits described in text, Sec. V B [(a), long-dash line; (b), short-dash line; (c), dotted line; (d), solid line].

interlayer interaction may be introduced in an approximate way via a mean-field correction to the ideal 2D susceptibility. The general form of such a correction is[14]

$$\chi(\text{cor})=\chi/[1-(2z'J'/Ng^2\mu_B^2)\chi] , \quad (5)$$

where z' and J' are the number of effective neighbors to a given manganese ion in adjacent layers and the associated interlayer interaction per pair of ions. The effect of a ferromagnetic interlayer exchange ($J'>0$) will be to enhance χ, and that of antiferromagnetic exchange to diminish it, relative to the uncorrected value. Consideration of the structure suggests that each manganese ion can perhaps interact, via a Mn—N—C—S $\cdots$ S—Mn-type interlayer-superexchange pathway (see Sec. VI), with four other manganese ions, two in each of the adjacent layers. Thus $z'=4$. Substituting this and other appropriate numerical values into Eq. (5), one finds the coefficient of χ in the denominator to be $5.333(J'/k)$ mole/emu K. Equation (5) is a reasonable way to incorporate J' provided the latter is substantially less than J, in this case therefore only a few 0.1 K at most. Thus, the magnitude of the coefficient (≈1) and the magnitude of χ itself (≈0.1 emu/mole) are such that only about a 10% effect on $\chi(T)$ should result. Moreover, for an antiferromagnetic susceptibility (the initial 2D-model prediction), χ does not vary dramatically in size between, in this case, 10 and 30 K. Therefore the shape of $\chi(T)$ in this region will not be very much altered, and one can anticipate that the location of the maximum, $T(\chi_{\max})$, will be little affected. It seems reasonable then that, rather than allowing both J and J' to vary in the fitting process, one should fix J at a value consistent with $T(\chi_{\max})$, namely $J/k=-0.70$ K, and fit only J', keeping g also fixed at 2.00, of course.

The results of such an approach are that in the 11–50-K range $\chi(T)$ is fit to an rms deviation of 0.62% with $J'/k=-0.23_8$ K; see Fig. 8. Including data to 300 K in the fit leads to a roughly similar value for the interlayer exchange, $J'/k=-0.27_0$ K, but a much poorer rms de-

viation of 3.6%; the deterioration is analogous to that noticed in fits not involving J'. In Fig. 8 we show for comparison purpose the calculated $\chi(T)$ for four sets of parameters: (a) $g=2.00$ and $J/k=-0.70$ K, as estimated from $T(\chi_{\max})$ alone assuming an ideal 2D-Heisenberg model; (b) $g=2.00$ and $J/k=-0.81_7$ K, from the 11–50-K HTSE fit assuming an ideal 2D-Heisenberg model; (c) $g=1.91_6$ and $J/k=-0.73_6$ K, from the same but allowing g to vary in the fit; and (d) $g=2.00$, $J/k=-0.70$ K, and $J'/k=-0.23_8$ K, as just described. In case (d) we note that $J'/J=0.34$, implying that the interlayer exchange is about a third as strong as the intralayer. If one does fit both J and J', with $g=2.00$ fixed, the result is very little different ($J/k=-0.69_1$ K, $J'/k=-0.25_3$ K, rms deviation=0.58%) from the best fit with J/k fixed at -0.70 K.

Certainly one striking feature of the susceptibility data is the very substantial uniaxial anisotropy in the paramagnetic region, which becomes increasingly apparent below about 30 K. Two common sources of anisotropy in a noncubic system are zero-field splittings due to single-ion anisotropy and magnetic dipole-dipole interactions. Another potential source of anisotropy, anisotropic exchange, is not expected to be significant for an orbitally nondegenerate Mn^{2+} system. Uniaxial single-ion anisotropy of the form $D[\hat{S}_z^2-S(S+1)/3]$ will lead to a splitting of the ground sextet (for $S=\frac{5}{2}$) of $6|D|$, with the high-M_s Kramers doublet low lying if $D<0$ and high if $D>0$. The susceptibility can be calculated for a field applied parallel and perpendicular to the z axis of the above interaction Hamiltonian. For $T\gg|D/k|$ the limiting forms are

$$\chi_{\parallel}=[N_0 g_{\parallel}^2\mu_B^2 S(S+1)/3kT](1-32D/15kT)$$

and

$$\chi_{\perp}=[N_0 g_{\perp}^2\mu_B^2 S(S+1)/3kT](1+16D/15kT)$$

(Ref. 15). If the anisotropy in the g value is negligible, as expected for a Mn^{2+} system, the anisotropy $\chi_{\parallel}-\chi_{\perp}$ is found to be

$$\Delta\chi=[N_0 g^2\mu_B^2 S(S+1)/3kT](-48D/15kT)\ . \qquad (6)$$

It is evident that for $D>0$, $\chi_{\perp}$ is greater than $\chi_{\parallel}$, and the reverse is true for $D<0$. The sign of D may not be determined unambiguously, since the choice of anisotropy axis, with respect to which $\chi_{\parallel}$ is referenced, influences it. From the data in Fig. 5 it is natural to assume that χ_{a^*} corresponds approximately to a unique $\chi_{\parallel}$, larger than $\chi_b\approx\chi_c$ which correspond to $\chi_{\perp}$. This requires $D<0$ in Eq. (6), and it is found that the temperature dependence of the anisotropy $\chi_{a^*}-\chi_c$ can be fairly well accounted for with $D/k=-0.14_5\pm0.008$ K. However, a problem of interpretation arises, for $\chi_{\parallel}$ (and $\chi_{\perp}$) are referred to a single-ion anisotropy axis z, which is most naturally associated with one of the bond axes in the coordination sphere of a Mn^{2+} ion. These are the O—Mn—O′, S—Mn—S′, and N″—Mn—N‴ axes of Fig. 1. None of these axes is particularly close to a^*, though O—Mn—O′ is the closest at about 48.5°. Moreover, there are two inequivalent pairs of manganese complexes in the unit cell, with two different sets of local coordination axis directions. The crystallographic direction a^* bisects the angle between the O—Mn—O′ axis of one pair and the O—Mn—O′ axis of the inequivalent pair. If one refines the analysis to take account of this fact, one finds that χ_{a^*} is a mixture of $\chi_{\parallel}$ and $\chi_{\perp}$ single-ion principal susceptibilities, and similarly for χ_c. Detailed analysis leads to $\chi_{a^*}-\chi_c=0.41(\chi_{\parallel}-\chi_{\perp})$. Thus the observed anisotropy is substantially less than the true single-ion anisotropy, and one might estimate that the value of D is rather on the order of $-0.35_5\pm0.020$ K. However, an inconsistency appears at this point. On the above assumptions χ_b should not be very similar to χ_c, contrary to observation. One is forced therefore to look for a different assignment of single-ion anisotropy.

The assignment which works best is to assume that N″—Mn—N‴, rather than O—Mn—O′, is the single-ion anisotropy axis. This direction is about 79.3° from a^*, 48.9° from b, and 43.0° from c. A $D>0$ will tend to direct the spin perpendicular to N″—Mn—N‴ and will make $\chi_{\perp}>\chi_{\parallel}$ according to Eq. (6). Since a^* is nearly perpendicular to N″—Mn—N‴, a large χ_{a^*} identifiable as essentially a $\chi_{\perp}$ can result. Detailed analysis leads to $\chi_{a^*}-\chi_c=0.50(\chi_{\perp}-\chi_{\parallel})$, so that the true D value is positive and twice as large as that shown in Fig. 9, where the more naive identification of χ_{a^*} with $\chi_{\perp}$ and χ_c with $\chi_{\parallel}$ is made. Moreover, on these assumptions χ_b and χ_c are calculated to be very similar, as observed, each being an approximately equal weight mixture of single-ion principal susceptibilities $\chi_{\parallel}$ and $\chi_{\perp}$. We conclude then that N″—Mn—N‴ is the single-ion anisotropy axis with $D/k=0.29\pm0.02$ K.

Since the anisotropy is significant below 25 K, it is arguable that the powder susceptibility, despite its less well formed maximum, is most suitable for fitting, because the effects of single-ion anisotropy cancel in a random

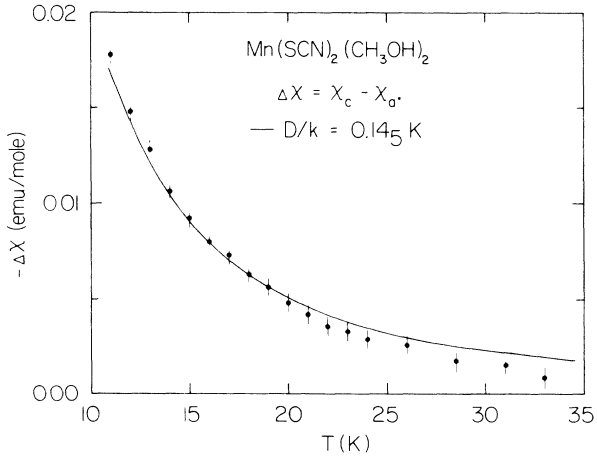

FIG. 9. Molar susceptibility anisotropy vs temperature for $Mn(SCN)_2(CH_3OH)_2$, and a fit based on the effects of zero-field splitting, with $\chi_c=\chi_{\parallel}$ and $\chi_{a^*}=\chi_{\perp}$ assumed. See Sec. V B of text for refinement of this analysis and corrected D value.

powder. As with the χ_c fits described previously, allowing g to vary in the analysis of powder data leads to excellent fits but also to unrealistically low g values. Fixing $g=2.00$ and neglecting interlayer exchange, use of the HTSE Eq. (4) leads to a best-fit (rms deviation=2.0%) value of $J/k=-0.78_0$ K employing 11–50 data; the result is shown in Fig. 10. Extending the fit to 300 K leads to a best-fit (rms deviation=2.3%) value of $J/k=-0.78_7$ K, virtually the same. It is apparent from Fig. 10 that similar defects occur here as when χ_c was treated this way, in particular, the position of the maximum is not very well reproduced. The value of J/k emerging from the powder fit is also only a few percent different from that obtained when fitting χ_c under similar conditions ($J/k=-0.81_7$ K).

In view of the discrepancy in $T(\chi_{\max})$ it is natural again, as with the χ_c data earlier, to introduce interlayer exchange via the mean-field formula Eq. (5), and to fix $g=2.00$ and $J/k=-0.70$ K also, in order to reproduce $T(\chi_{\max})=12.6$ K. Fitting in the 11–50-K range yields $J'/k=-0.16_2$ K with an rms deviation of 0.2%; this also appears in Fig. 10. Extending the fit to 300 K yields only a slightly different value, $J'/k=-0.17_1$ K, with an rms deviation of 1.0%. One notes that somewhat smaller rms deviations have been obtained in fits to powder data than when fitting χ_c earlier. The interlayer-exchange interaction is still antiferromagnetic however, and of the same general magnitude as before, being about one-third smaller in size.

The result $|J/k|=0.37\pm0.02$ K inferred from the temperature dependence of the low-field magnetization in Sec. V A should be interpreted as a mean value of the exchange interaction in $Mn(SCN)_2(CH_3OH)_2$. If one calculates such a mean value from the results of fitting the powder susceptibility in the preceding paragraph, the result is

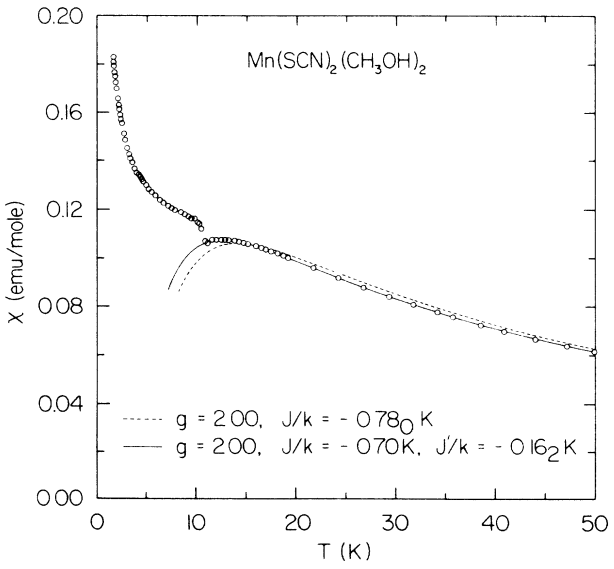

FIG. 10. Molar susceptibility vs temperature for polycrystalline $Mn(SCN)_2(CH_3OH)_2$, and theoretical fits described in text. Applied magnetic field is 2400 G.

$$J/k=[4(-0.70\text{ K})+4(-0.16\text{ K})]/8=-0.43\text{ K},$$

where $z=4$ and $z'=4$ were assumed. The susceptibility fitting results should be more reliable, but clearly, within the limitations of the theories employed, the agreement between these estimates is excellent.

C. Possible spin reorientation

An obvious feature of the susceptibility data is the upturn at low temperatures along each axis. The presence of paramagnetic impurities, not uncommon in Mn^{2+} systems, naturally suggests itself. An attempt was made to subtract the theoretical $\chi(T)$ from the observed $\chi(T)$ and to test whether the difference, $\Delta\chi$, conformed to a Curie law, $\Delta\chi=C'/T$, or Curie-Weiss law, $\Delta\chi=C'/(T-\Theta')$. This did not work well for either χ_c or χ (powder), at least partly because the theoretical $\chi(T)$, a monotonic decrease to zero value at 0 K for temperatures below $T(\chi_{\max})$, does not correspond to what the observed susceptibilities would be even with impurity contributions subtracted out. That is, in this compound, as in $Mn(SCN)_2(C_2H_5OH)_2$ studied previously,[6] none of the crystal susceptibilities fall to zero at 0 K because there is no single axis of spin alignment. It may be preferable to base the analysis on χ_{a^*} instead, which is more akin to a perpendicular susceptibility. For 2D antiferromagnets especially, $\chi_\perp(T)$ often shows a pronounced minimum at some temperature near or a bit below T_c.[1(a),16] An attempt to model χ_{a^*} as the sum of such a $\chi_\perp(T)$ and χ (impurity)$=C'/(T-\Theta')$ appeared to give plausible results, with $C'=0.03_4$ emu K mole^{-1} (corresponding to an impurity content of about 0.8%) and $\Theta'=1.2_0$ K. However, a very strong objection to an impurity-based explanation of the low-temperature susceptibility upturn is that no such effect is seen in the low-field data of Fig. 6. Moreover, no such major paramagnetic impurity effects were seen in the low-field susceptibility data on $Mn(SCN)_2(C_2H_5OH)_2$,[6] prepared by the same method employed here for the methanol system. It seems much more likely then that the low-temperature upturns, perhaps anticipatory of the 3.7_5 K anomaly in the same data, are intrinsic. They may arise from some subtle spin reorientation process occurring in fields of sufficient strength. We are unable to say more than this.

VI. DISCUSSION

A. 2D character and ordering temperature

Some alternative attempts at accounting for the observed susceptibility of $Mn(SCN)_2(CH_3OH)_2$ in terms of a 2D Heisenberg model were displayed in Figs. 8 and 10. For the χ_c data, fits (a) and (b) suffer from rather obvious defects already noted. Fit (c) looks very good, but the fitted g value is dubiously low. Fit (d) is fairly attractive, but has the drawback that the calculated susceptibility is slightly larger than the actual data between about 11 and 8 K. With regard to (c), one might speculate that a weighing error could be responsible. But χ scales as g^2, and the value $g=1.916$, 4.2% less than 2.00, requires an

8.2% overestimate of the mass. This is too large to be credible in view of the care that was taken. Moreover, the average of χ_b, χ_c, and χ_{a^*} is in reasonable agreement with the powder susceptibility. Since $g=1.916$ is unacceptably low for a Mn^{2+} compound, fit (d),with $g=2.00$ and incorporating a significant antiferromagnetic interlayer exchange, would appear to be preferable. In view of the apparent strength of this interaction, a considerable degree of 3D character should occur, and the situation may be describable in terms of a 2D to 3D crossover. For a given antiferromagnetic exchange strength, the susceptibility is smaller for a 3D than for a 2D system, because of the additional antiferromagnetic correlations. Of course, a mean-field correction to account for this cannot reproduce fine points of the behavior, especially near the ordering temperature, here 10.5 K. One may anticipate that, relative to the mean-field correction, $\chi(T)$ will drop more sharply on the low-temperature side of χ_{max} as the transition is approached, as is observed. An acceptable fit to the powder data also requires the introduction of antiferromagnetic interlayer exchange, as represented by the solid curve in Fig. 10.

Given the substantial ratio $J'/J=0.34$ from fit (d) to χ_c, or even $J'/J=0.23$ from the powder fit, one may ask whether a 3D model might be more appropriate in the first instance, discounting the apparent implications of the crystal structure. One can obtain some perspective on this by comparing the results on applying Eqs. (2) and (3), for the 2D (square-planar) Heisenberg model with $S=\frac{5}{2}$, with analogous results obtained for the $S=\frac{5}{2}$ 3D (body-centered cubic) Heisenberg model. The bcc lattice, with eight interacting neighbors, appears appropriate for comparison, as it is topologically similar to the situation in $Mn(SCN)_2(CH_3OH)_2$ where $z=4$ and $z'=4$, for a total of eight interacting neighbors. The predictions for this model are[17]

$$kT(\chi_{max})/|J|S(S+1)=4.18\pm0.09\ , \tag{7}$$

$$\chi_{max}|J|/N_0g^2\mu_B^2=0.0301\ . \tag{8}$$

Employing the observed values of $T(\chi_{max})$ and χ_{max} given earlier, one estimates from Eq. (7) that $J/k=-0.34_4\pm0.014$ K, and from Eq. (8) that $J/k=-0.43_9\pm0.004$ K. The two estimates differ by 21.6%. The discrepancy between the values emerging from Eqs. (2) and (3), -0.70 K and -0.80 K, is 12.5%. Though imperfect, the consistency is obviously better in the 2D case.

An attempt was also made to fit the powder data using a HTSE for the three-dimensional, $S=\frac{5}{2}$, Heisenberg antiferromagnet (AF), though only the series for the simple cubic (sc) lattice (not the most appropriate) is available in suitable form.[18] The resulting 11–50-K fit, with $g=2.00$ fixed, $J/k=-0.55_8$ K, and rms deviation=1.2%, was somewhat better than that for the pure 2D model (without J'), the dashed curve in Fig. 10, but not nearly so good as that for the 2D model with J', the solid curve in Fig. 10. To avoid cluttering the diagram, and because we do not believe this model to be really appropriate, the 3D curve is not shown in Fig. 10.

For 3D Heisenberg AF's the ordering temperature is typically just a bit less than $T(\chi_{max})$. Thus for the $S=\frac{5}{2}$ bcc model mentioned in connection with Eqs. (7) and (8), $T_c/T(\chi_{max})=0.967$.[17] Even for the low coordination number sc lattice, this ratio is a relatively high 0.925.[17] For 3D Ising AF's the situation is similar, with $T_c/T(\chi_{max})=0.939$ and 0.911 for the bcc and sc lattices, respectively.[19] For 2D AF's the ratio is much smaller, for example 0.651 for the 2D Ising AF on a square planar lattice.[20] For 2D Heisenberg AF's a transition to long-range order does not occur in the absence of at least some small anisotropy or interlayer exchange, so that definite predictions for $T_c/T(\chi_{max})$ cannot be made in the absence of specific details. However, $S=\frac{5}{2}$ 2D Heisenberg AF's rather typically have ordering temperatures such that $T_c/|J/k|$ is in the range 9–11.[1(a)] From Eq. (2) one finds that $T(\chi_{max})=17.9_4|J/k|$. In other words, the observed ordering generally occurs at a temperature about 50% lower than that of the maximum in χ. Clearly, the situation in $Mn(SCN)_2(CH_3OH)_2$, with $T_c/T(\chi_{max})=0.83$, is not nearly so extreme. Presumably a combination of both interlayer exchange and anisotropy increases the ratio substantially, though the value is still well below those for genuine 3D systems. For the previously studied $Mn(SCN)_2(C_2H_5OH)_2$, which displays much less anisotropy and which presumably has much weaker interlayer exchange, $T_c/T(\chi_{max})=10.3$ K/14.5 K=0.71, a value in somewhat better conformity with 2D model expectations.

One can also approach the T_c question in the following way. A lower limit on the transition temperature in the case of an ideal 2D Heisenberg antiferromagnet can be estimated as the theoretical Stanley-Kaplan temperature, where the susceptibility (staggered for an antiferromagnet) is predicted to diverge even though no long-range order develops (as proved rigorously by Mermin and Wagner[21]). This temperature is[22]

$$T_{SK}=(z-1)[2S(S+1)-1]|J/k|/5\ . \tag{9}$$

Substituting $J/k=-0.80$ K, the mean of best values obtained with a realistic $g=2.00$ and assuming a strictly 2D model with $z=4$, there results $T_{SK}=7.9$ K for $Mn(SCN)_2(CH_3OH)_2$. In any real system there will be at least some interlayer exchange and/or anisotropy present, and this will lead to a genuine transition to long-range order at a temperature a bit higher than T_{SK}. The ratio in the case of $Mn(SCN)_2(CH_3OH)_2$ is $T_c/T_{SK}=1.33$. For the related $Mn(SCN)_2(C_2H_5OH)_2$, with $J/k=-0.88$ K and $T_c=10.3$ K, the ratio is 1.18. The latter is somewhat similar to the ratio for Rb_2MnF_4 (1.16) and somewhat larger than the ratio for K_2MnF_4 (1.11).[16] The ratio for the present system is exceptionally large, because of relatively strong interlayer exchange and anisotropy.

The ratio $T_c/|\Theta|$ can sometimes also be informative. The Weiss constant Θ is given by mean-field theory as $2zS(S+1)J/3k$, and will tend to agree better with experimental values when, as is usual for mean-field results, the spin is large. This ratio tends to be found in the range 0.31–0.48 for actual 2D Heisenberg AF's with $S=\frac{5}{2}$, but

in the range of 0.69–0.79 for actual 3D Heisenberg AF's with the same spin.[1(a)] Theoretical predictions for the ratio are similar, e.g., 0.72 for the $S=\frac{5}{2}$ simple cubic case.[23] If we use this formula with $J/k=-0.80$ K, there results $\Theta=-18.7$ K, within 17% of the observed $\Theta=-22.4$ K. The ratio $T_c/|\Theta|$ is 0.56 if we use the calculated Θ, and 0.47 if we use the observed Θ, values that are certainly more 2D-like than 3D-like. For the probably more nearly ideal 2D system $Mn(SCN)_2(C_2H_5OH)_2$ one calculates $\Theta=-20.5$ K, in excellent agreement with the observed $\Theta=-20.9$ K. The ratio $T_c/|\Theta|=0.49$–0.50 conforms well with 2D expectations.

B. Anisotropy and canting mechanism

From an analysis of the paramagnetic anisotropy in $Mn(SCN)_2(CH_3OH)_2$ it was concluded in Sec. V B that the anisotropy axis was N″—Mn—N‴ with $D/k=0.29$ K, a substantially larger magnitude value than would seem to occur for $Mn(SCN)_2(C_2H_5OH)_2$. It is well known that the zero-field splitting parameter D is sensitive to even small distortions of the immediate coordination sphere of the paramagnetic ion.[24,25] Although we cannot predict what the specific dependence will be, it is worth noting that the Mn-S distance 2.733 Å in $Mn(SCN)_2(CH_3OH)_2$ is 1.6% longer than in $Mn(SCN)_2(C_2H_5OH)_2$, while the Mn-O and Mn-N distances are 0.6% and 0.4% shorter, respectively, in the methanol compound. Although small, these variations may be sufficient to influence D appreciably, especially as it is a small parameter to begin with in a Mn^{2+} compound. Still, the value found here for D is rather large for such systems, where values of a few 0.01 K are more typical.[1(b),26] However, an even larger magnitude value, $D/k=-0.529$ K, has been reported for $[(CH_3)_3NH]MnBr_3\cdot 2H_2O$,[27] in which an O—Mn—O′ axis is suggested as the anisotropy axis. In this lower dimensional (1D) system, as in ours, the anisotropy in g is believed to be too small to contribute significantly to the anisotropy in χ, but the effects of short-range order may also be a source of anisotropy. Magnetic dipole-dipole interactions probably also make a small contribution to the total anisotropy in $[(CH_3)_3NH]MnBr_3\cdot 2H_2O$, where the smallest Mn-Mn separation is only 3.79 Å, as they are believed to do in some other Mn^{2+} systems where the Mn-Mn separations are of the order 4 Å.[16,28,29] But in $Mn(SCN)_2(CH_3OH)_2$ the smallest Mn-Mn separation is 5.927 Å; nor are there dramatic differences between this and the next-nearest-neighbor and next-next-nearest-neighbor distances. By comparison with dipole-dipole anisotropy effects in the other manganese systems cited, we estimate that no more than about a 0.001-emu/mole anisotropy in χ arises from this interaction even at 10 K. Much the predominant source of the observed anisotropy in our compound is the zero-field splitting. The effects of short-range order above T_c are probably responsible for the small departures, evident in Fig. 9, from the predicted T^{-2} dependence of $\Delta\chi$.

In Sec. V A the angle by which the spins are canted from the c axis was determined to be 0.20°. This fairly small canting angle is also typical of manganese systems, where the sources of anisotropy which can lead to spin canting are usually small. Two mechanisms can be operative in this regard: antisymmetric exchange of the form $\hat{\mathcal{H}}'_{ex}=\mathbf{d}_{ij}\cdot[\hat{\mathbf{S}}_i\hat{\mathbf{S}}_j]$, and crystal-field anisotropy or g-tensor anisotropy that is differently oriented (inequivalent) at different magnetic sites in the unit cell.[30] In order for either mechanism to operate it is necessary that there be no inversion center between the magnetic sites. This condition is fulfilled for $Mn(SCN)_2(CH_3OH)_2$. There are four manganese ions in the unit cell which divide into two pairs, the two ions in each pair being connected by inversion, but with no inversion center between the pairs. Normally at least some small anisotropy in the g tensor is needed for either mechanism to be efficacious. This is because $d_{ij}\propto(g-2)/g$ in the case of antisymmetric exchange,[30] while inequivalent site anisotropy may not occur if the g tensor is fully symmetric. However, in the present case there is also single-ion anisotropy from the zero-field splitting which is tied to the N″—Mn—N‴ coordination axis. The directions of this axis for the two pairs indicated above are 82.2° apart. This inequivalence alone might lead to spin canting; certainly any additional $E[\hat{S}_x^2-\hat{S}_y^2]$ term that might be present could also contribute, somewhat as occurs for NiF_2.[31,32]

It seems very probable that it is the single-ion anisotropy rather than antisymmetric exchange which is responsible for the spin canting in $Mn(SCN)_2(CH_3OH)_2$. The order of magnitude of d_{ij} is $J(g-2)/g$, while the lowest energy canted spin arrangement is characterized by $\phi\approx|d/2J|$.[30] Taking $\phi=0.20°$ and $J/k=-0.80$ K, one estimates that a g anisotropy of the order 0.014 is required. No EPR measurements are available to test this, and the susceptibility measurements are not quite precise enough to distinguish a 0.5% anisotropy in g; however, it would be very surprising if such a large Δg occurred, since in Mn^{2+} systems any such effects are typically an order of magnitude smaller, i.e., $\Delta g\approx 0.001$. On the other hand, given the large axial anisotropy characterized by $D/k=0.29$ K, along with a possible secondary orthorhombic anisotropy term for which E may be as large as $|D/3|$,[33] it is quite plausible that a canting angle of 0.20° might result. This angle is proportional to the ratio of the anisotropy constant to the exchange constant,[31,32] and in NiF_2, with a canting angle of 0.76°, the ratios are only a few times larger than in $Mn(SCN)_2(CH_3OH)_2$. The canting angle which has been inferred for the related compound $Mn(SCN)_2(C_2H_5OH)_2$, approximately 10°,[6] is we believe far too large. This was not a direct determination however. Independent measurements of our own indicate that the spontaneous magnetization of the weak ferromagnetic moment in the ethanol compound is of very similar magnitude to that in the methanol, so that the canting angle should also be quite similar.

C. Magnetostructural correlations and comparison with ethanol homologue

The dominant intralayer-exchange interaction which has emerged here for $Mn(SCN)_2(CH_3OH)_2$, $J/k=-0.70$ K, is somewhat more weakly antiferromagnetic than that

found previously for $Mn(SCN)_2(C_2H_5OH)_2$, $J/k = -0.88$ K. It is of interest to consider whether this difference can be rationalized on structural grounds. Initially, the result may seem surprising, since as noted in Sec. III the near-neighbor and next-nearest-neighbor intralayer manganese ion separations are a bit smaller in the methanol system than in the ethanol. All else being equal, the strength of a superexchange interaction though a given bridging ligand is expected to decrease as the separation of magnetic centers increases. Separation is not, however, the only relevant variable, and there are certain features present here which work in the opposite direction. The SCN^- group is essentially identical in length and degree of linearity in the two systems, being perhaps 0.3% shorter and 0.3° nearer linearity in $Mn(SCN)_2(C_2H_5OH)_2$; but the differences are within the experimental uncertainties. More significant perhaps is the fact that the Mn—S distance in the methanol system is 2.733 Å but is 2.691 Å in the ethanol. Although at the other end of the bridge the Mn—N distance is slightly shorter in the methanol, 2.135 Å versus 2.143 Å in the ethanol system, the difference in Mn—S distance is much more substantial. This should tend to weaken, if only slightly, the interaction in the methanol system relative to the ethanol. Probably more important, however, are the angular variables along the Mn—S—C—N—Mn bridge. In $Mn(SCN)_2(CH_3OH)_2$ the Mn—S—C angle is 99.4°, and the C—N—Mn angle is 164.0°; in $Mn(SCN)_2(C_2H_5OH)_2$ these angles are 103.6° and 169.0°, respectively. Although apparently small, these angular differences are significant. It is well established that the magnitude and sign of an exchange interaction via a single atom bridge are very sensitive to the bridging angle.[34] Thus, the results of Hatfield, Hodgson, and co-workers on a series of symmetrically bibridged Cu(II) hydroxide complexes indicate that the exchange interaction between copper ions varies from a strongly positive (ferromagnetic) value of 100 cm^{-1} to a strongly negative (antiferromagnetic) value of -100 cm^{-1} as the bridging angle varies from 95° to 100°, and becomes much more negative for even larger angles, the dependence on angle being linear to 105° anyway.[35]

Similar dependences have been observed for chloride bridges, the interaction again becoming more antiferromagnetic as the bridging angle increases. In the case of polynuclear bridges, a description of the situation would necessarily be more complex, and certainly fewer systematic magnetostructural correlation data are available on which to base conclusions. Worth noting, however, are the results of Duggan and Hendrickson on a series of Ni(II) complexes bibridged by N_3^-, NCO^-, NCS^-, and $NCSe^-$ groups.[36] For example, the N—N—Ni angle is 135° in the azide bridged complex and the interaction is antiferromagnetic; in the thiocyanate bridged complex the C—S—Ni angle is 90° and the interaction is ferromagnetic. Again, a trend toward a more antiferromagnetic interaction as a characteristic angle in the bridge increases is evident. It seems very likely that the somewhat smaller angles involved in the Mn—S—C—N—Mn bridges of the methanol system are the principal factors responsible for the somewhat weaker antiferromagnetic intralayer-exchange interaction in this system relative to its ethanol homologue. Such angular dependences have become increasingly understandable in light of recent theories of ligand mediated exchange interactions between metal ions.[37]

Apart from the thiocyanate linkages, there is one other exchange path which probably operates between manganese ions in a layer. This is a hydrogen bond to a sulfur from a neighboring coordination sphere, Mn—O—$H_0 \cdots$ S—Mn. Distances in this path are as follows: Mn—O, 2.165 Å; O—H_0, 0.78 (±0.07) Å; $H_0 \cdots$ S, 2.54 (±0.07) Å; and S—Mn, 2.733 Å. Some associated angles are Mn—O—H_0, 113 (±5)° and O—H_0—S, 155 (±5)°. For comparison, in $Mn(SCN)_2(C_2H_5OH)_2$ the corresponding distances are as follows: Mn—O, 2.177 Å, O—H_0, 0.85 (±0.05) Å; $H_0 \cdots$ S, 2.43 (±0.05) Å; and S—Mn, 2.691 Å. Associated angles are Mn—O—H_0, 120 (±3)° and O—H_0—S, 166 (±4)°. The O—H_0 bond length appears to be significantly shorter in the methanol system than in the ethanol, but there is a large uncertainty in this distance for both systems. Conversely, the $H_0 \cdots$ S distance is significantly larger in the methanol system than in the ethanol, again with substantial uncertainties in these distances. It seems likely that the total path length for this exchange circuit is somewhat longer for the methanol system, while the angular variables are somewhat larger (more nearly linear) for the ethanol system. The former comparison should tend to make the H-bonding exchange interaction relatively weaker in the methanol compound, the latter should tend to make it relatively more antiferromagnetic in the ethanol compound. Exchange interactions through hydrogen bonds can be quite efficient,[36] and the interactions discussed above may make a significant contribution to the total intralayer interaction in these systems.

Some observations can also be made concerning interlayer-exchange interactions in $Mn(SCN)_2(CH_3OH)_2$. As noted in Sec. III, the nearest-neighbor manganese ions in adjacent layers are 7.817 Å apart, a substantially larger separation than the two smallest intralayer separations. No less important is the absence of intimate bonding connections between the layers, as Figs. 2 and 3 illustrate rather clearly. However, there are interlayer S $\cdots$ S separations worth considering. The shortest of these is 3.964 Å, the next shortest 4.807 Å. The van der Waals radius of sulfur is commonly taken as 1.85 Å.[38] Hence, the shortest interlayer sulfur-sulfur separation is 7.1% larger than the van der Waals contact distance. This suggests that some small interlayer interaction may occur, via a Mn—S $\cdots$ S—C—N—Mn pathway. There appears to be some indication of this in the significantly improved susceptibility fit on incorporating a mean-field correction for interlayer exchange. Angular variables along this pathway should also be important. The Mn—N—C angle is 164.0°, the NCS group is essentially linear, the C—S $\cdots$ S angle is 148.7° and the S $\cdots$ S—Mn angle is 111.0°. The predominance of large angles along this pathway suggests that the resultant interlayer exchange is probably antiferromagnetic. The results of the susceptibility fitting support this.

No interlayer exchange was considered in the susceptibility fits previously reported for $Mn(SCN)_2(C_2H_5OH)_2$. Structural considerations suggest that any interlayer exchange should be much weaker in the ethanol system. The manganese layers are substantially farther apart, 8.507 Å versus 7.222 Å in the methanol system. Furthermore, the sulfur atoms do not lie quite so far out of the manganese layer in the ethanol system, displacements from this plane being 1.68 Å versus 1.92 Å in the methanol system. Thus, interlayer sulfur-sulfur separations are not less than 5.14 Å in $Mn(SCN)_2(C_2H_5OH)_2$, a value much greater than twice the van der Waals radius.

VII. CONCLUSIONS

Analysis of its structural properties and magnetic behavior shows that $Mn(SCN)_2(CH_3OH)_2$ is describable as a quasi-2D Heisenberg antiferromagnet, though one in which significant interlayer coupling also occurs. The intralayer-exchange interaction is $J/k = -0.70(3)$ K,and the interlayer-exchange interaction is $J'/k = -0.16(2)$ K, as deduced from susceptibility data. These values are also consistent with a mean antiferromagnetic exchange interaction $|J/k| = 0.37(2)$ K estimated from the temperature dependence of the low-field magnetization due to the weak ferromagnetic moment along the monoclinic b axis. Analysis of the observed anisotropy in the single-crystal susceptibility yields a zero-field splitting parameter $D/k = 0.29(2)$ K, with the z axis of the single-ion anisotropy term $D\hat{S}_z^2$ along the N″—Mn—N‴ coordination axis. The material becomes antiferromagnetically ordered at 10.5(2) K, with c the probable easy axis and with the spins canted 0.20° towards b. The canting is due to inequivalent site anisotropy in combination with the zero-field splitting, rather than to antisymmetric exchange interaction. Magnetic dipole-dipole interactions are not an important source of anisotropy, though they may contribute, along with an $E[\hat{S}_x^2 - \hat{S}_y^2]$ orthorhombic anisotropy term, to the emergence of c as the easy axis. There is some evidence for a spin reorientation transition near 3.75 K, though the details are not resolved.

The ratio of the observed ordering temperature $T_c = 10.5$ K to $T(\chi_{max}) = 12.6$ K is 0.83, and suggests that the system is of lattice dimensionality intermediate between two and three. It is certainly less ideally two-dimensional than the previously studied ethanol homologue. Also, the ratio of T_c to the theoretical Stanley-Kaplan temperature for an ideal 2D Heisenberg antiferromagnet is 1.33, which is higher than for most good two-dimensional systems. Still, the ratio $T_c/|\Theta| \approx 0.50$ is definitely more 2D-like than 3D-like.

The fact that the antiferromagnetic intralayer-exchange interaction in $Mn(SCN)_2(CH_3OH)_2$ is somewhat weaker than that in $Mn(SCN)_2(C_2H_5OH)_2$, can be understood in terms of the detailed superexchange pathways in the two systems. Differences in angular variables along these pathways (primarily Mn—S—C—N—Mn) are more important than differences in interatomic distances. The somewhat smaller angles along the polynuclear SCN^- bridges in the methanol system, and also along an intralayer Mn—O—H · · · S—Mn hydrogen bond pathway, should tend to make the superexchange interactions less strongly antiferromagnetic in $Mn(SCN)_2(CH_3OH)_2$ than in $Mn(SCN)_2(C_2H_5OH)_2$, as observed. The much stronger interlayer-exchange interaction in the methanol system than in the ethanol is more simply explained by the significant sulfur-sulfur interlayer overlaps occurring in the former but not in the latter. That the interlayer interaction is antiferromagnetic is also easily explained by the angular variables along this interlayer Mn—S · · · S—C—N—Mn superexchange pathway.

ACKNOWLEDGMENTS

This work was supported by National Science Foundation—Solid State Chemistry—Grant No. DMR-8906337 and by the Petroleum Research Fund of the American Chemical Society.

[1]See, e.g., (a) L. J. de Jongh and A. R. Miedema, Adv. Phys. **23**, 1 (1974); (b) R. L. Carlin, *Magnetochemistry* (Springer-Verlag, Berlin, 1986).

[2]See, e.g., *Organic and Inorganic Low-Dimensional Crystalline Materials,* Vol. 168 of *NATO Advanced Study Institute, Series B: Physics,* P. Delhaes and M. Drillon (Plenum, New York, 1987).

[3]G. C. DeFotis, C. K. Barlowe, and W. R. Shangraw, J. Magn. Magn. Mater. **54–57**, 1493 (1986).

[4]G. C. DeFotis, E. M. McGhee, K. R. Echols, and R. S. Wiese, J. Appl. Phys. **63**, 3569 (1988).

[5]G. C. DeFotis, B. T. Wimberly, and E. M. McGhee, J. Phys. (Paris) Colloq. **49**, C8-855 (1988).

[6]J. N. McElearney, L. L. Balagot, J. A. Muir, and R. D. Spence, Phys. Rev. B **19**, 306 (1979).

[7]C. D. Flint and M. Goodgame, J. Chem. Soc. A **442** (1970).

[8]G. C. DeFotis, B. K. Failon, F. V. Wells, and H. H. Wickman, Phys. Rev. B **29**, 3795 (1984).

[9]Cynthia S. Day (unpublished).

[10]*International Tables for X-ray Crsytallography* (Kynoch, Birmingham, 1967), Vol. I; *International Tables for X-ray Crystallography* (Kynoch, Birmingham, 1969), Vol. II; *International Tables for X-ray Crystallography* (Kynoch, Birmingham, 1974), Vol. IV.

[11]M. E. Fisher, Philos. Mag. **7**, 1731 (1962).

[12]T. Oguchi, Phys. Rev. **117**, 117 (1960).

[13]M. E. Lines, J. Phys. Chem. Solids **31**, 101 (1970).

[14]J. W. Stout and W. B. Hadley, J. Chem. Phys. **40**, 55 (1964); J. N. McElearney, D. B. Losee, S. Merchant, and R. L. Carlin, Phys. Rev. B **7**, 3314 (1973).

[15]B. Bleaney, Phys. Rev. **78**, 214 (1950); B. Bleaney and D. J. E. Ingram, Proc. R. Soc. London, Ser. A **205**, 336 (1951).

[16]D. J. Breed, Physica **37**, 35 (1967).

[17]J. A. Puertolas, R. Navarro, F. Palacio, J. Bartolome, D. Gonzalez, and R. L. Carlin, Phys. Rev. B **26**, 395 (1982).

[18]L. J. de Jongh and D. J. Breed, Solid State Commun. **15**, 1061 (1974).

[19]M. E. Fisher and M. F. Sykes, Physica **28**, 939 (1962).

[20]M. F. Sykes and M. E. Fisher, Physica **28**, 919 (1962).
[21]N. D. Mermin and H. Wagner, Phys. Rev. Lett. **17**, 1133 (1966).
[22]H. E. Stanley and T. A. Kaplan, Phys. Rev. Lett. **17**, 913 (1966).
[23]G. S. Rushbrooke and P. J. Wood, Mol. Phys. **6**, 409 (1963).
[24]Y. Ajiro, S. A. Friedberg, and N. S. Vander Ven, Phys. Rev. B **12**, 39 (1975).
[25]W. M. Walsh, Jr., Phys. Rev. **114**, 1473 (1959).
[26]C. J. Ballhausen, *Introduction to Ligand Field Theory* (McGraw-Hill, New York, 1962), p. 247.
[27]I. Yammamoto and K. Nagata, J. Phys. Soc. Jpn. **43**, 1581 (1977).
[28]T. Smith and S. A. Friedberg, Phys. Rev. **176**, 660 (1968).
[29]J. N. McElearney, Inorg. Chem. **17**, 248 (1978).
[30]T. Moriya, in *Magnetism*, edited by G. T. Rado and H. Suhl (Academic, New York, 1963), Vol. 1.
[31]T. Moriya, Phys. Rev. **117**, 635 (1960).
[32]A. H. Cooke, K. A. Gehring, and R. Lazenby, Proc. Phys. Soc. London **85**, 967 (1965).
[33]H. H. Wickman, M. P. Klein, and D. A. Shirley, J. Chem. Phys. **42**, 2113 (1965).
[34]R. D. Willett, in *Magneto-Structural Correlation in Exchange Coupled Systems*, edited by R. D. Willett, D. Gatteschi, and O. Kahn (Reidel, Dordrecht, 1985), p. 389.
[35]V. H. Crawford, H. W. Richardson, J. R. Wasson, D. J. Hodgson, and W. E. Hatfield, Inorg. Chem. **15**, 2107 (1976).
[36]D. N. Hendrickson, in *Magneto-Structural Correlation in Exchange Coupled Systems*, Ref. 34, p. 523.
[37]P. J. Hay, J. C. Thibeault, and R. Hoffmann, J. Am. Chem. Soc. **97**, 4884 (1975).
[38]L. Pauling, *The Nature of the Chemical Bond*, 3rd ed. (Cornell University Press, Ithaca, 1960), p. 260.